Chapter 10

Advanced Accretion Disks

The total luminosity of a disk with the viscous dissipation rate $D(R)$ is

$$L_{\rm disk} = 2\pi \int_{R_*}^{\infty} D(R) R dR = \frac{1}{2} \frac{G M_* \dot{M}}{R_*} \ . \tag{10.1}$$

The disk luminosity is *half* of the total accretion luminosity $L_{\rm acc} = G M_* \dot{M}/R_*$; the other half of the luminosity is emitted when the gas makes the transition from the inner edge of the accretion disk to the surface of the compact object. The physical characteristics of the **boundary layer** between the Keplerian disk and the compact object are poorly known. Let's start by considering the better-known luminosity that comes from the disk itself.

If the disk is optically thick, and the luminosity $L_{\rm disk}$ is in the form of black body radiation, then the temperature $T_{bb}(R)$ at a given radius is set by the relation

$$\sigma_{SB} T_{bb}^4 = \frac{1}{2} D(R) \ . \tag{10.2}$$

The factor of $1/2$ enters because we are considering the radiation from only one side of the disk. Using $D(R)$ for a viscous accretion disk,

$$T_{bb}(R) = T_* \left(\frac{R}{R_*} \right)^{-3/4} [1 - (R_*/R)^{1/2}]^{1/4} \ , \tag{10.3}$$

where

$$T_* = \left(\frac{3 G M_* \dot{M}}{8\pi R_*^3 \sigma_{SB}} \right)^{1/4} \ . \tag{10.4}$$

The temperature of the disk is plotted in Figure 10.1. The hottest part of

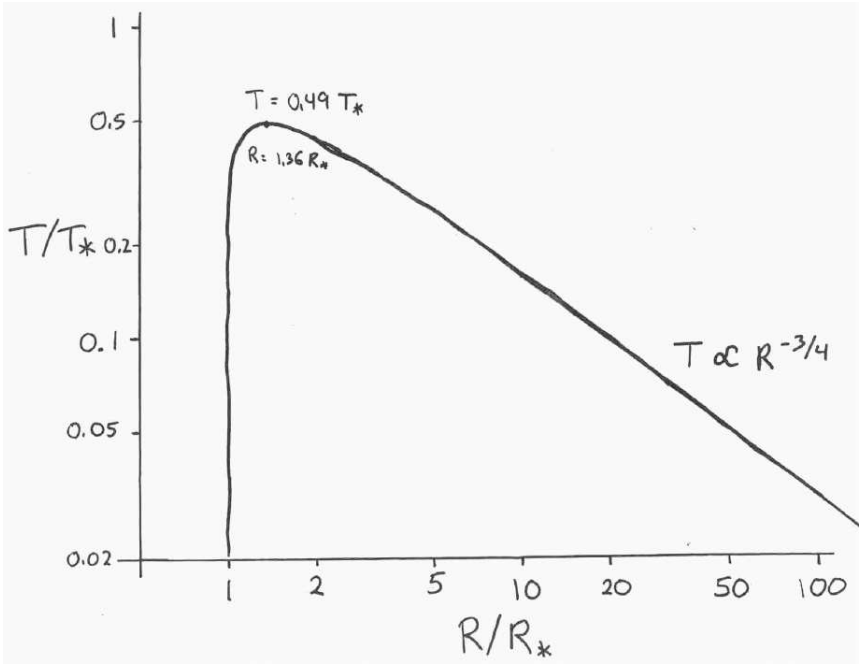

Figure 10.1: The temperature of an optically thick accretion disk.

the disk is at $R = 1.36R_*$, where $T_{bb} = 0.488T_*$. The characteristic disk temperature T_*, for typical X-ray binaries, is

$$T_* = 1 \times 10^7 \,\mathrm{K} \left(\frac{\dot{M}}{10^{17}\,\mathrm{g\,sec^{-1}}}\right)^{1/4} \left(\frac{M_*}{1\,\mathrm{M_\odot}}\right)^{1/4} \left(\frac{R_*}{10\,\mathrm{km}}\right)^{-3/4} . \qquad (10.5)$$

The spectrum of the disk is the black-body spectrum integrated over all radii:

$$S_\nu \propto \int_{R_*}^{R_o} \frac{\nu^3}{\exp[h\nu/kT_{bb}(R)] - 1} RdR \ , \qquad (10.6)$$

where R_o is the outer radius of the accretion disk. At high frequencies, $\nu \gg kT_*/h$, the spectrum falls away exponentially. At lower frequencies, $\nu \ll kT_*/h$, the temperature has the radial dependence $T \propto R^{-3/4}$, and the spectrum has the form

$$S_\nu = \nu^{1/3} \int_0^{h\nu/kT_o} \frac{x^{5/3}dx}{e^x - 1} \ . \qquad (10.7)$$

When $kT_o/h \ll \nu \ll kT_*/h$, the upper limit of the integral may be taken as infinity, yielding the spectrum $S_\nu \propto \nu^{1/3}$ at intermediate frequencies. At very low frequencies, $\nu \ll kT_o/h$, the main contribution to the spectrum is the Rayleigh-Jeans tail of the cool, outer edge of the accretion disk; the resulting frequency dependence is $S_\nu \propto \nu^2$. The integrated spectrum S_ν for a disk with $T_* = 100T_o$ is plotted in Figure 10.2.

One check to see whether the 'physically thin, optically thick' model is correct is to check for the characteristic $\nu^{1/3}$ spectrum. Unfortunately, in binary systems, the luminosity of the normal star that is providing the accreting matter may overpower the luminosity of the disk. The best system for seeing the entire spectrum of the accretion disk is a cataclysmic variable in which the compact star is a white dwarf and the normal star is a low mass ($0.1 \rightarrow 1\,\mathrm{M_\odot}$) main sequence star. In the quiescent state, between cataclysmic outbursts, most of the luminosity comes from the disk. The cataclysmic variable VW Hydri (a dwarf nova) has a very dim normal companion, and a large disk. The observed spectrum of VW Hydri, in its post-outburst state, is shown in Figure 10.3. It is a fairly good example of a $\nu^{1/3}$ law.

It is enlightening to do slightly more elaborate modeling of alpha disks, to find its properties as a function of the radius R, the mass M_* of the central object, the accretion rate $\dot{M}$, and the assumed value of α. Let ρ, a, P, and

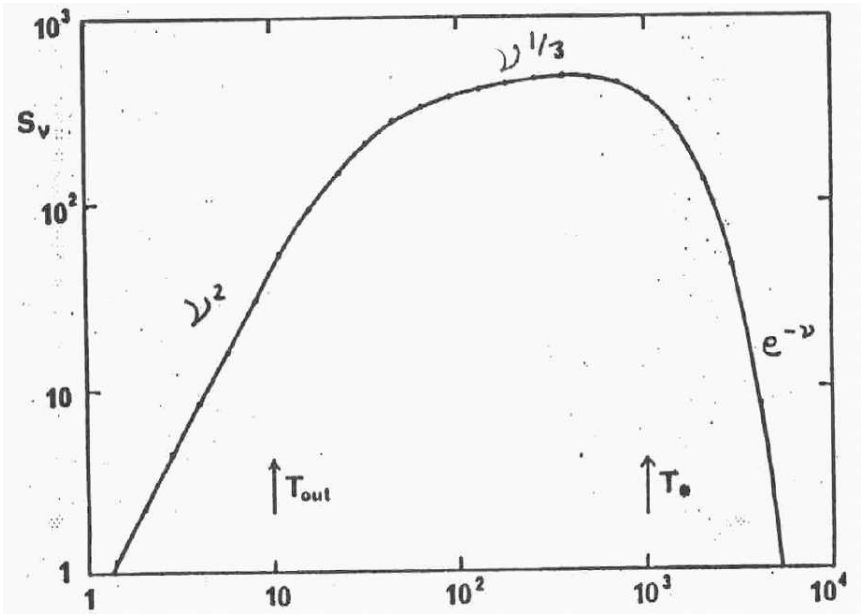

Figure 10.2: The spectrum S_ν of an optically thick accretion disk. The units of ν and S_ν are arbitrary. The temperature at the outer edge of the disk is $T_{\rm out} = T_o = 0.01 T_*$.

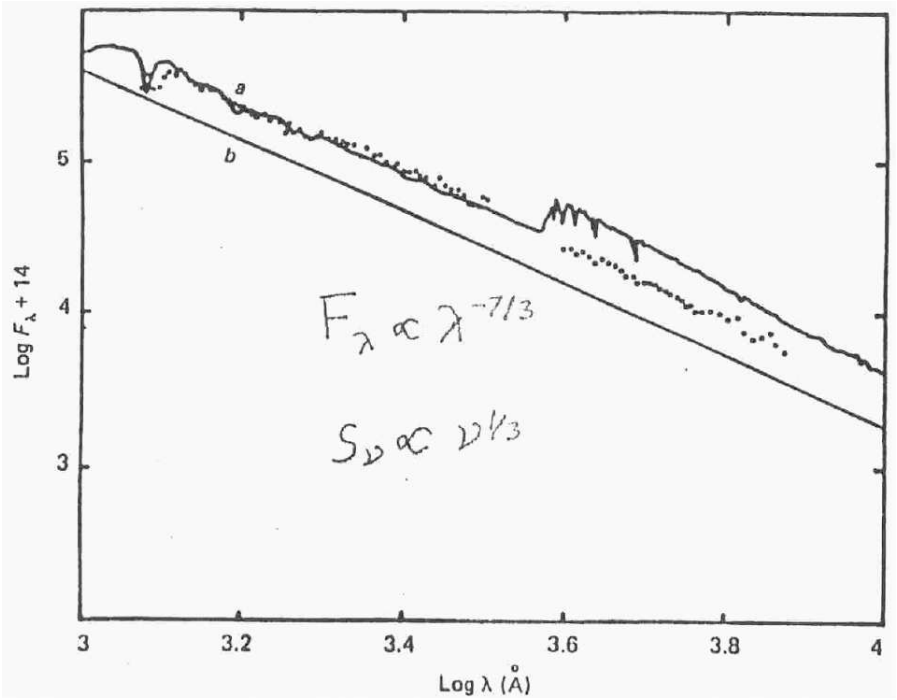

Figure 10.3: The dots are the observed spectrum F_λ of VW Hydri after an outburst. Line 'a' is a stellar atmosphere fit; line 'b' is a line of slope $F_\lambda \propto \lambda^{-7/3}$, corresponding to $S_\lambda \propto \nu^{1/3}$.

T be the density, sound speed, pressure, and temperature in the $z = 0$ plane. The optical depth $\tau = \rho H \kappa_R$ of the disk (where κ_R is the Rosseland mean opacity) is assumed to be much greater than one. We can solve for the eight unknowns ρ, Σ, H, a, P, T, τ, and ν as a function of M_*, $\dot{M}$, R, and α. Equations for the alpha disk:

$$\rho = \frac{\Sigma}{H} \tag{10.8}$$

$$H = a \left(\frac{R^3}{GM_*} \right)^{1/2} \tag{10.9}$$

$$a^2 = \frac{P}{\rho} \tag{10.10}$$

$$P = \frac{\rho k T}{m} \tag{10.11}$$

$$\frac{4\sigma_{SB} T^4}{3\tau} = \frac{3GM_*\dot{M}}{8\pi R^3} \left[1 - \left(\frac{R_*}{R} \right)^{1/2} \right] \tag{10.12}$$

$$\tau = \Sigma \kappa_R(\rho, T) \tag{10.13}$$

$$\nu\Sigma = \frac{\dot{M}}{3\pi} \left[1 - \left(\frac{R_*}{R} \right)^{1/2} \right] \tag{10.14}$$

$$\nu = \alpha a H \tag{10.15}$$

When the dominant source of opacity in the disk is free-free absorption, the Rosseland mean opacity $\kappa_R(\rho, T)$ is well approximated by Kramers' law:

$$\kappa_R = 6.6 \,\mathrm{cm^2\,g^{-1}} \left(\frac{\rho}{10^{-8}\,\mathrm{g\,cm^{-3}}} \right) \left(\frac{T}{10^4\,\mathrm{K}} \right)^{-7/2} . \tag{10.16}$$

At higher temperatures and lower densities, the main source of opacity is Thomson scattering of photons by free electrons, with $\kappa_R = 0.40\,\mathrm{cm^2\,g^{-1}}$.

The above set of equations has an algebraic solution. Let $f \equiv 1 - (R_*/R)^{1/2}$, $R_{10} \equiv R/10^{10}\,\mathrm{cm}$, $M_c \equiv M_*/1\,\mathrm{M_\odot}$, and $\dot{M}_{16} \equiv \dot{M}/10^{16}\,\mathrm{g\,s^{-1}}$. If the dominant source of opacity is free-free absorption, then

$$\Sigma = 5\,\mathrm{g\,cm^{-2}}\,\alpha^{-4/5} \dot{M}_{16}^{7/10} M_c^{1/4} R_{10}^{-3/4} f^{14/5} \tag{10.17}$$

$$H = 2 \times 10^8\,\mathrm{cm}\,\alpha^{-1/10} \dot{M}_{16}^{3/20} M_c^{-3/8} R_{10}^{9/8} f^{3/5} \tag{10.18}$$

$$\rho = 3 \times 10^{-8}\,\mathrm{g\,cm^{-3}}\,\alpha^{-7/10} \dot{M}_{16}^{11/20} M_c^{5/8} R_{10}^{-15/8} f^{11/5} \tag{10.19}$$

$$T = 1 \times 10^4 \,\mathrm{K}\, \alpha^{-1/5} \dot{M}_{16}^{3/10} M_c^{1/4} R_{10}^{-3/4} f^{6/5} \tag{10.20}$$

$$\tau = 30\, \alpha^{-4/5} \dot{M}_{16}^{1/5} f^{4/5} \tag{10.21}$$

$$\nu = 2 \times 10^{14}\, \mathrm{cm}^2\, \mathrm{sec}^{-1}\ \alpha^{4/5} \dot{M}_{16}^{3/10} M_c^{-1/4} R_{10}^{3/4} f^{6/5} \tag{10.22}$$

$$u_R = 3 \times 10^4\, \mathrm{cm\,s}^{-1}\, \alpha^{4/5} \dot{M}_{16}^{3/10} M_c^{-1/4} R_{10}^{-1/4} f^{-14/5}\ . \tag{10.23}$$

Fortunately, none of these results have an exorbitantly strong dependence on the unknown value of α.

We can check whether our assumption of Kramers' law is valid. The opacity within the disk will be

$$\kappa_R(\mathrm{Kramers}) = 6.3\, \mathrm{cm}^2\, \mathrm{g}^{-1}\ \dot{M}_{16}^{-1/2} M_c^{-1/4} R_{10}^{3/4} f^{-2}\ . \tag{10.24}$$

The bremsstrahlung opacity dominates over the electron scattering opacity at radii

$$R > 2.5 \times 10^8\, \mathrm{cm}\, \dot{M}_{16}^{2/3} M_c^{1/3} f^{8/3}\ . \tag{10.25}$$

The crossover radius is smaller than the radius of a white dwarf for values of $\dot{M}$ typical of cataclysmic binaries. Thus, for white dwarfs, Kramers' law usually holds. In X-ray binaries with a central neutron star, the inner parts of the accretion disk will have an opacity dominated by electron scattering.

The boundary layer emits half the accretion luminosity. In the absence of a magnetic field, the accretion disk can extend all the way to the surface of the compact object, and the boundary layer consists of a very thin region just above the surface of the compact object. Consider the boundary layer in the accretion disk around a *non-magnetic* compact object of mass M_* and radius R_*. The boundary layer consists of the region $R_* < R < R_* + b$, where the angular velocity decreases from its Keplerian value

$$\Omega(R_* + b) = \left(\frac{GM_*}{(R_* + b)^3} \right)^{1/2} \tag{10.26}$$

to the angular velocity of the star's surface

$$\Omega_* < \left(\frac{GM_*}{R_*^3} \right)^{1/2}\ . \tag{10.27}$$

The angular velocity in the vicinity of the boundary region is plotted in Figure 10.4. The radial extent b of the boundary layer is less than the disk

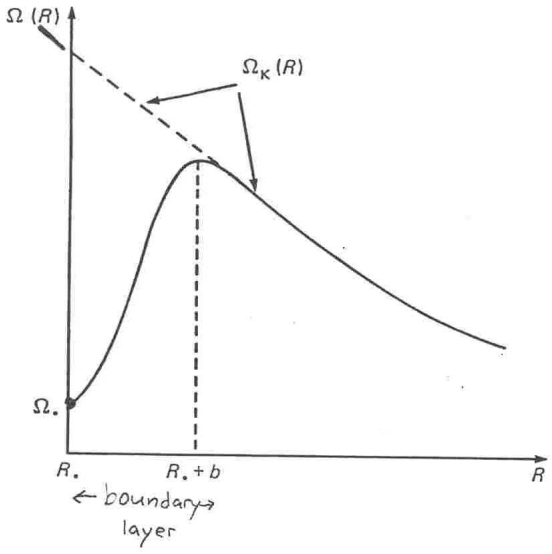

Figure 10.4: The distribution of angular velocity Ω in the boundary layer, compared to the Keplerian value.

thickness H just outside the boundary layer, which in turn is less than the radius R_* of the compact object. To show that $b < H < R_*$, start with the equation for conservation of radial momentum:

$$u_R \frac{\partial u_R}{\partial R} - \frac{u_\phi^2}{R} + \frac{1}{\rho}\frac{\partial P}{\partial R} + \frac{GM_*}{R^2} = 0 \ . \tag{10.28}$$

In the Keplerian disk, the gravitational term (GM_*/R^2) is balanced by the centrifugal term (u_ϕ^2/R). Within the boundary layer, the gravitational term is balanced by the pressure gradient term. The magnitude of the pressure gradient is

$$\frac{1}{\rho}\frac{\partial P}{\partial R} \sim \frac{a^2}{b} \ , \tag{10.29}$$

where a is the sound speed at the outer edge of the boundary layer and b is the thickness of the boundary layer. From the balance of forces, $a^2/b \sim GM_*/(R_* + b)^2$, we see that

$$b \sim \frac{R_* + b}{M_\phi^2} \ , \tag{10.30}$$

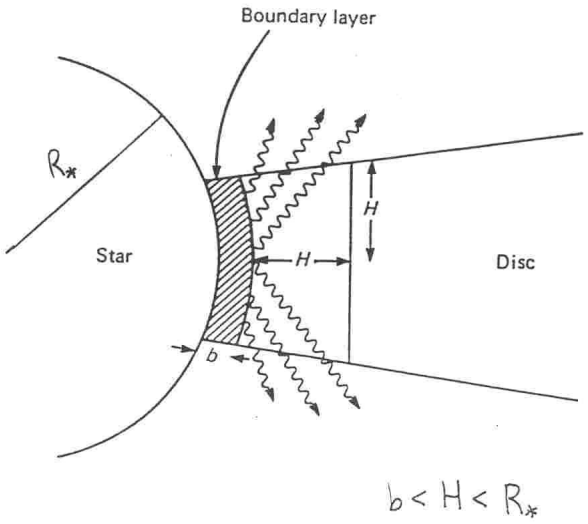

Figure 10.5: A sketch of the boundary layer of an optically thick disk.

where M_ϕ is the rotational Mach number at the outer edge of the boundary layer. In a thin disk, $M_\phi \gg 1$, and $H \sim R/M_\phi$, so $b \sim H/M_\phi \sim R_*/M_\phi^2$. Figure 10.5 shows the resulting geometry, with $b \ll H \ll R_*$. The blackbody temperature within the boundary layer is

$$T_{BL} \approx M_\phi^{1/4} T_* \ . \tag{10.31}$$

Magnetic fields can affect the accretion of matter. The magnetic field of compact stars is a dipole field, with dipole moment $\mu = B_* R_*^3$, where R_* is the radius of the star and B_* is the magnetic field at the surface of the star. A neutron star typically will have $R_* \approx 10^6\,\mathrm{cm}$ and $B_* \approx 10^{12}\,\mathrm{G}$, yielding $\mu = 10^{30}\,\mathrm{G\,cm^3}$. A white dwarf with $R_* \approx 5 \times 10^8\,\mathrm{cm}$ and $B_* \approx 10^4\,\mathrm{G}$ will have the same magnetic moment, $\mu \approx 10^{30}\,\mathrm{G\,cm^3}$.

At distances $r \gg R_*$, the amplitude of the dipole magnetic field is

$$B \approx \frac{\mu(1 + 3\cos^2\theta)^{1/2}}{r^3} \ , \tag{10.32}$$

where θ is angle measured from the magnetic pole. The magnetic energy density in the equatorial plane is

$$E_{\rm mag} = \frac{B^2}{4\pi} = \frac{1}{4\pi}\frac{\mu^2}{r^6} \approx 8 \times 10^{22}\,\mathrm{erg\,cm^{-3}}\ \mu_{30}^2 R_6^{-6} \left(\frac{r}{R_*}\right)^{-6} \ . \tag{10.33}$$

The quantity μ_{30} is the magnetic moment of the star, measured in units of $10^{30}\,\mathrm{G\,cm^3}$; the quantity R_6 is the radius R_* of the star, measured in units of $10^6\,\mathrm{cm}$.

Consider a neutron star or white dwarf isolated in the middle of a uniform gaseous medium. The accreting matter will fall in radially at large distances, where the magnetic pressure is small. The infall will be significantly deflected from a radial flow at a radius r_A (the **Alfven radius**), where the magnetic energy density $E_{\rm mag}$ is equal to the kinetic energy density $E_{\rm kin}$ of the gas. From the continuity equation,

$$\rho u = -\frac{\dot{M}}{4\pi r^2} \ . \tag{10.34}$$

For an ionized gas ($\gamma = 5/3$) inside the accretion radius, the infall velocity is

$$u = -\left(\frac{GM_*}{2r}\right)^{1/2} \ . \tag{10.35}$$

The kinetic energy density is thus

$$E_{\rm kin} = \frac{1}{2}\rho u^2 = \frac{\dot{M}\sqrt{GM_*}}{8\pi\sqrt{2}} r^{-5/2} \ . \tag{10.36}$$

The Alfven radius is

$$r_A \approx \left(\frac{\mu^4}{\dot{M}^2 G M_*}\right)^{1/7} \ . \tag{10.37}$$

Using the appropriate numerical values for a neutron star or white dwarf,

$$r_A = 7\times 10^8\,\mathrm{cm}\,\mu_{30}^{4/7}\dot{M}_{16}^{-2/7}M_c^{-1/7} \ . \tag{10.38}$$

Accreting neutron stars will generally have $r_A \gg R_*$. A typical white dwarf will have $r_A \sim R_*$.

There exists, however, a class of *magnetic white dwarfs*, which have magnetic dipole moments as large as $\mu \sim 10^{34}\,\mathrm{G\,cm^3}$, and Alfven radii $r_A \sim 10^{11}\,\mathrm{cm}$. One class of cataclysmic variables, known as AM Herculis systems, consists of magnetic white dwarfs with low mass main sequence companions, on an orbit with $P \lesssim 3\,\mathrm{hr}$. In these systems, the Alfven radius is larger than the orbital radius. The mass that is lost by the main sequence star is compelled to flow along the magnetic field lines.

Consider a binary system in which the magnetic field of the compact star is small enough to allow an accretion disk to form. The accretion disk will be disrupted at a radius R_A, which is the radius at which the torque exerted by the magnetic field on the disk is equal to the viscous torque. Computing the magnetic torque is, unfortunately, difficult. The torque exerted depends on the azimuthal component B_ϕ of the magnetic field, which in turn depends on the extent to which the magnetic dipole configuration is distorted by the interaction of the magnetic field with the disk. Calculations usually show that $R_A \approx r_A/2$.

Because the magnetic field lines are pinned to the compact object, they have an angular velocity equal to Ω_*, the angular velocity with which the compact object rotates. At radii $R \geq R_A$, the accreting gas rotates with an angular velocity $\Omega(R) = (GM_*/R^3)^{1/2}$. At radii $R \leq R_A$, the gas flows along the magnetic field lines, and hence rotates with an angular velocity $\Omega(R) = \Omega_*$. For steady accretion to occur, we must have a situation in which $\Omega_* \leq (GM_*/R_A^3)^{1/2}$. Numerically, this requires that

$$\Omega_* < 2\,\mathrm{sec}^{-1}\ \mu_{30}^{-6/7} \dot{M}_{16}^{3/7} M_c^{5/7}\ . \tag{10.39}$$

If the magnetized compact object rotates more rapidly than this, gas will be unable to accrete.

Matter will leave the accretion disk at a radius R_A and flow along the magnetic field lines to the magnetic poles of the neutron star, as shown in Figure 10.6. The rotation axis of the the neutron star is aligned with the rotation axis of the disk. However, the magnetic axis of the neutron star is generally at an angle to the rotation axis of the disk. Let α be the angle between the magnetic axis of the star and the plane of the disk, as shown in Figure 10.6. In polar coordinates (r, θ) aligned with the magnetic axis, the magnetic field lines are described by the equation $r(\theta) = C \sin^2\theta$. The field line that passes through the disk at the radius $r = R_A$ and angle $\theta = \alpha$ must then have the equation

$$r(\theta) = R_A \frac{\sin^2\theta}{\sin^2\alpha}\ . \tag{10.40}$$

The gas that is ripped away from the disk will follow along this path until it reaches the surface of the neutron star at a radius $r = R_*$. The accretion thus takes place on a ring of angular radius θ_c around the magnetic pole, where θ_c is given by the relation

$$\sin^2\theta_c = \frac{R_*}{R_A}\sin^2\alpha\ . \tag{10.41}$$

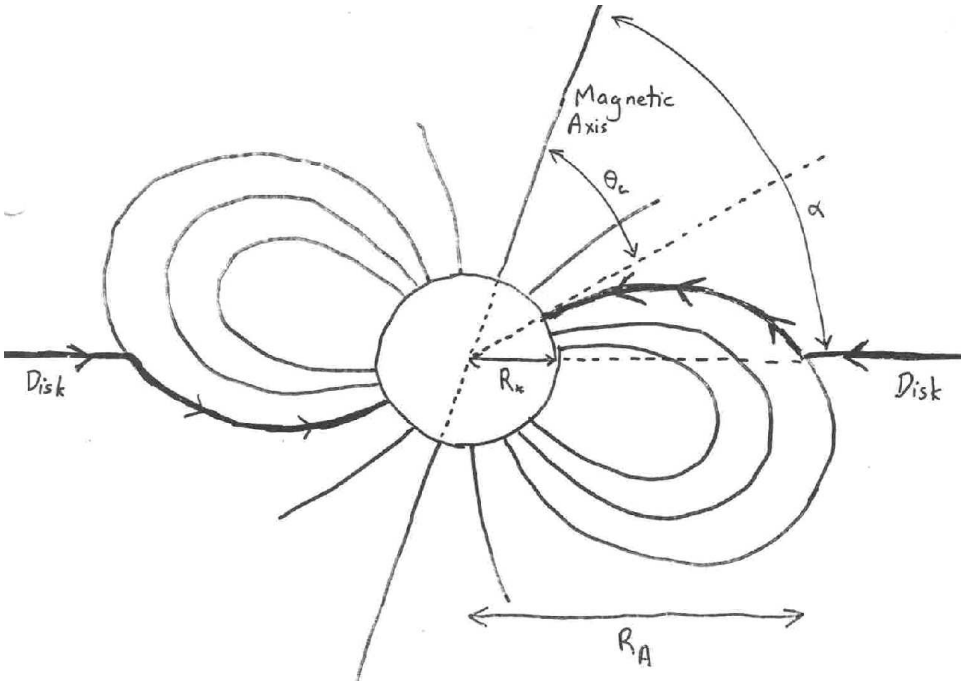

Figure 10.6: Accretion from a gaseous disk onto a magnetized neutron star.

Diffusion effects tend to smear the area of accretion into a circular cap centered on the magnetic pole. The area of the two accreting polar caps takes up a fraction

$$f \sim 2\frac{\pi R_*^2 \sin^2\theta_c}{4\pi R_*^2} \sim \frac{R_* \sin^2\alpha}{2R_A} \tag{10.42}$$

of the total surface area of the neutron star. The fraction f is small; $f \sim 10^{-3}$ for a neutron star with $\alpha \sim \pi/2$. All of the 'boundary layer' accretion luminosity, equal in value to $L = (GM_*\dot{M})/(2R_*)$, will be emitted from two small regions. The rotation of the neutron star will cause a periodic modulation in the observed flux from the accreting polecaps. Pulsation periods are observed in X-ray binaries, with typical periods in the range $1\,\mathrm{sec} \lesssim P \lesssim 10^3\,\mathrm{sec}$. In many X-ray binaries, the pulsation period P is observed to be decreasing steadily, on time scales of $\sim 10^4\,\mathrm{yr}$. This spin-up is the result of the torque exerted by the accretion disk on the magnetic field of the neutron star. For a magnetized neutron star accreting matter from a disk, the Keplerian angular velocity at the Alfven radius, $\Omega = (GM_*/R_A^3)^{1/2}$, is larger than Ω_*, the angular velocity of the neutron star and its attached magnetic field. The star + magnetic field combination is thus accreting angular momentum from the disk at the rate $\dot{M}R_A^2\Omega(R_A)$. If the moment of inertia of the star is $I \sim M_*R_*^2$, then the spin-up rate is given by the relation

$$I\dot{\Omega}_* = \dot{M}R_A^2\Omega(R_A) = \dot{M}(GM_*R_A)^{1/2}\ . \tag{10.43}$$

The spin-up rate for the neutron-star is then

$$-\frac{\dot{P}}{P} \approx 10^{-5}\,\mathrm{yr}^{-1}\, I_{45}^{-1}\dot{M}_{16}^{6/7}\mu_{30}^{2/7}M_c^{3/7}P_1\ , \tag{10.44}$$

where I_{45} is the moment of inertia in units of $10^{45}\,\mathrm{g\,cm^2}$.